Some technological aspects regarding laser ablation of oxides resulting from exposing alloyed steels to high temperatures

M. SELAGEA[a,*], E. MORARU[a,*], D. BESNEA[a,*], R. UDREA[b], B. LUNGU[a,b]
[a]*Politehnica University of Bucharest, Bucharest 060042, Romania*
[b]*Apel Laser SRL, Mogosoaia, 077135, Romania*

The use of alloyed steels in industry to fabricate different parts and components has become increasingly common. This is due to their high resistance to oxidation and corrosion. In the vast majority of cases, the oxide layer has a protective role, generally against corrosion. However, for the fabrication of certain products, some of the manufacturing steps require the removal of these oxides, both as a pre-processing step and as a post-processing step, depending on the functional role of the respective component / product. The removal of this oxide layer can be determined by the requirements of the product appearance and/or the functional aspects of the product. The aim of this paper is to determine the optimal process parameters for removing these oxides by laser ablation, without causing structural and tribological changes of the material, regardless of it being a pre- or post-processing method.

(Received April 9, 2019; accepted October 9, 2019)

Keywords: Laser ablation, Oxides, Fiber Laser, Scanner

1. Introduction

The laser has found its place in many of the industry's fields of activity, for applications like laser welding or surface treatment. Its importance is growing year by year [1-13]. Alloyed steel processing for the execution of products or components by conventional, electrical welding, but also by other processes (such as TIG –Tungsten Inert Gas) involves the formation of oxides that in many cases have to be eliminated. This type of welding has been chosen because it allows the welding of materials with small thicknesses and is very common in welding of alloyed steel. The elimination of these oxides can be accomplished by several methods, for example by mechanical processes (involving reduced installation and consumable costs, however the process is cannot be controlled and a poor surface finish is produced) or by chemical and electrochemical processes (which have the disadvantages of using toxic substances, being slow and requiring many operations). Laser cleaning by ablation is a process commonly found in many industrial segments: aeronautics, automotive, for selective material removal, for example: rust, oils, paints, plastics and polymers. In this case, the laser cleaning machine will be used to remove the oxides resulting from the high temperature exposure of 316 L stainless steel plates by realization of a welding seam with additive material by TIG process, using a 1.6 mm diameter ER308 LSI electrode.

Laser cleaning is the process by which contaminants, debris or impurities (e.g. carbon, silicon and rubber) are removed from the surface of a material by laser irradiation. This is an ecological and low-cost technology that is widely used throughout the industry on a global scale. The purpose is to remove contaminated coats and quickly clean the surface with a minimal amount of heat.

This is done using laser irradiation, which makes it a process similar to laser ablation. There are different ways of laser surface cleaning, which will be listed in the next section, along with various fiber-laser cleaning applications [14-18, 22].

2. Experimental

There are two different ways to perform fiber laser cleaning and choosing the process depends on the desired results. The first process is simply removing a layer from the surface of the material. The removed layer will be different from that of the piece physically and chemically, which means that the fiber laser will have no thermal, chemical or mechanical effect on the substrate. For example, paint or rubber coatings [22].

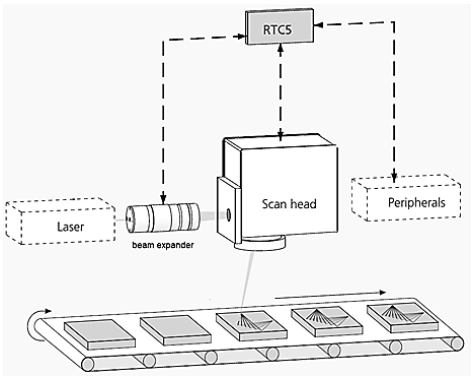

Fig. 1. Operating scheme of the laser cleaning machine used in this research [19]

The second process consists of decontaminating the surface with the laser. This involves removing layers that have penetrated deep into the structure of the object to be cleaned. Therefore, the layers of the substrate itself must be removed. One example is the removal of radioactive concrete layers. Fiber laser cleaning represents a non-contact technique, without chemicals or solvents. The process can be automated using robots and then used on a larger scale. These financial and ecological benefits make fiber laser cleaning extremely useful, because it maximizes efficiency and safety, while reducing waste. The laser machine used in this work has been integrated and assembled within the company Apel Laser SRL and has the following operating scheme, shown in Fig. 1.

The laser used is a solid-state, fiber:Yb laser, manufactured by IPG GmbH, model YLP-V2-1-100-20-20, having the following features, shown in Table 1.

Table 1. IPG's YLP-V2-1-100-20-20 fiber laser specs [20]

Specs	Min	Type	Max	Unit
Mode of operation		Pulsed		-
Polarization		Random		-
Max pulse energy		1		mJ
Nominal average output power	19	20	21	W
Output power adjustment	10		100	%
Pulse width	80	100	120	ns
Central emission wavelength	1055	1064	1075	nm
Repetition rate	2		200	kHz
Beam diameter	6		9	mm
Beam quality factor M^2			2	-

Table 2. Scanlab's SCANcube® 7 galvanometer specs [19]

Optical performance	
Gain error	<5 mrad
Zero offset	<5 mrad
Skew	<6 mrad
Nonlinearity	<3.5 mrad
Repeatability	<22 µrad
Long term drift > 8 hours	<0.3 mrad
Offset drift	<30 µrad/K
Gain drift	<80 ppm/K
Dynamic performance	
Tracking error	<0.14 ms
Typical positioning speed	75 rad/s
Maximum positioning speed	150 rad/s
Typical marking speed	2.5 m/s
Step response	0.3 – 0.7 ms
Mirrors	
Coating	Dielectric
Working wavelength	1064 nm
Reflectivity	99.5%(1064 nm)
Maximum allowed laser power	100 W
Maximum allowed power density	500 W/cm^2
Damage threshold for pulsed operation	5 J/cm^2

The laser beam is transported to the galvanometric scanner through an optical fiber to a collimation and conditioning telescope for the laser beam.

The simultaneous control of the laser and scanner is accomplished by the Real Time Control Board (RTC), the SL2-100 protocol for the galvanometric scanner with a 20-bit positioning resolution; laser control is achieved with a resolution of 15 ns, 20 mA and control of peripheral equipment is carried out with a resolution of 2-16 bits.

The design of experiments has been realized by taking into account the following parameters: average power (P), repetition rate (R_r), working speed (V), jump speed (V_J), pulse duration (τ), spot overlap (S_O), line spacing (L_S), number of passes (N), focal length (f), hatch type (H_T), work area (W_A) and spot diameter ($Ø$). Some of these will remain constant throughout the experiments, at least in the first phase: f=255 mm, W_A=30 x 20 mm . Another parameter that remains constant during the whole experiment is the spot diameter:

$$Ø = \frac{C \cdot \lambda \cdot f}{A} \quad (1)$$

where, C is a constant that relates to the degree of pupil illumination and input truncation (for a Gaussian beam, C = 1.83 when the entrance beam is truncated at the $1/e^2$ diameter); λ – laser beam wavelength, 1064 nm; A – diameter of the incident beam, 9 mm. According to equation (1), the resulting spot diameter is 70.9 µm.

In this case, 50% beam overlap will be used, so that the line spacing will be 35 µm and the working speed will be a function of spot diameter, overlap and work frequency, as follows:

$$V = Ø \cdot (1 - S_O) \cdot R_r \quad (2)$$

Initially, it starts at a repetition rate of 2 kHz, which will remain constant during the first 15 experiments, and thus determining the working speed, using equation (2): V=0.136 m/s [21, 23].

3. Results and discussions

Thus, in the first phase, the pulse duration will be varied for different levels of average optical output power. These results are shown in Table 3.

Table 3. First batch of tests

Avg. power (%)	Pulse width (ns)	Roughness (mm)
20	80	0.38
40		0.62
60		0.95
80		1.13
100		1.3
20	100	0.07
40		0.67
60		0.86
80		1.29
100		1.33
20	120	0.15
40		0.86
60		1.46
80		1.08
100		1.33

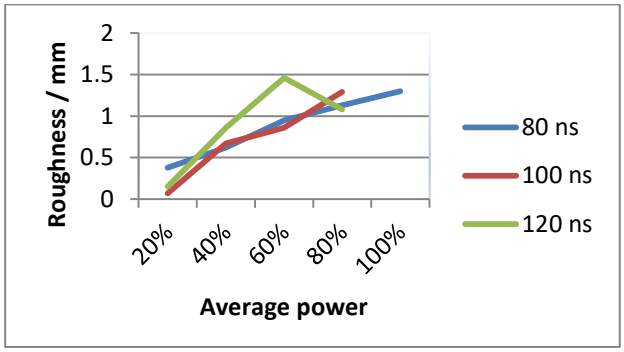

Fig. 2. Plot of average power vs. roughness for the first batch of tests

Considering these results, it was decided to impose the following conditions for the next batches: an average optical power below 40%, because, regardless of pulse duration, over this value the roughness exceeds the acceptable threshold. The cycle time, compared to the work area is high (167 seconds) and therefore the following batches varied in repetition rate, but no more than 37 kHz, so we do not exceed the working speed at which the scanner is stable, namely 2.5 m/sec.

The next test batches will reflect a variation of pulse repetition rate, thus a variation of working speed (without exceeding the speed at which the galvanometric scanner is stable). Each batch will be made at constant pulse duration (80ns/100ns/120ns).

Table 4. Results of varying R_r at τ=100 ns

R_r(kHz)	V(m/s)	V_J(m/s)	τ(ns)	P(%)	R_a(µm)
5	0.342	1.026	100	20	0.17
10	0.684	2.052			0.24
15	1.026	3.078			0.34
20	1.368	4.104			0.24
25	1.711	5.133			0.97
30	2.053	6.159			0.27
35	2.395	7.185			0.18
37	2.532	7.596			0.35

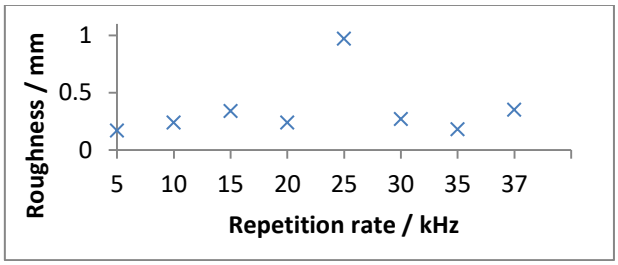

Fig. 3. Plot of R_a against R_r at τ=100 ns, P=20%

Table 5. Results of varying R_r at τ=120 ns, P=20%

R_r(kHz)	V(m/s)	V_J(m/s)	τ(ns)	P(%)	R_a(µm)
5	0.342	1.026	120	20	0.37
10	0.684	2.052			0.17
15	1.026	3.078			0.25
20	1.368	4.104			0.28
25	1.711	5.133			0.24
30	2.053	6.159			0.27
35	2.395	7.185			0.3

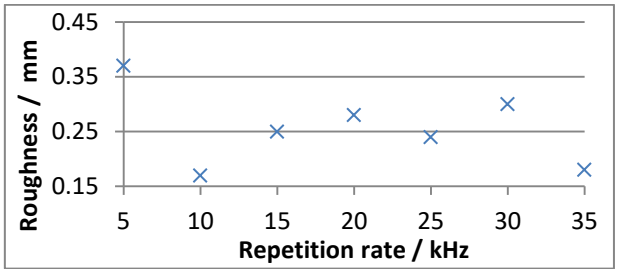

Fig. 4. Plot of R_a against R_r at τ=120 ns, P=20%

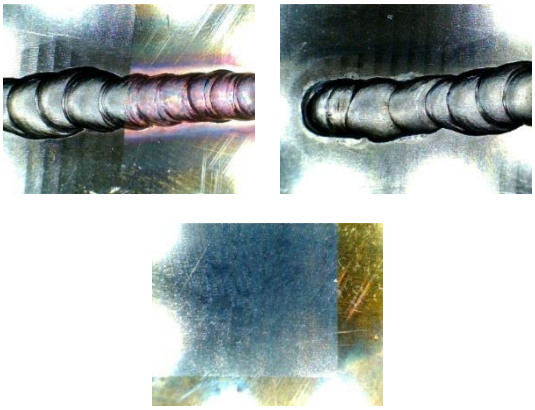

Fig. 5. Welding seam laser cleaned at f=2 kHz, τ=100 ns, P=20%, 20X magnification

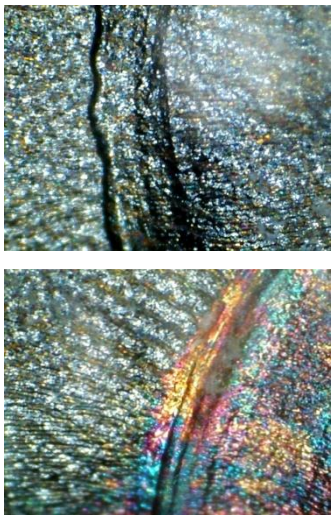

Fig. 6. Welding seam laser cleaned at f= 2 kHz, τ=100 ns, P=20%, 400X magnification

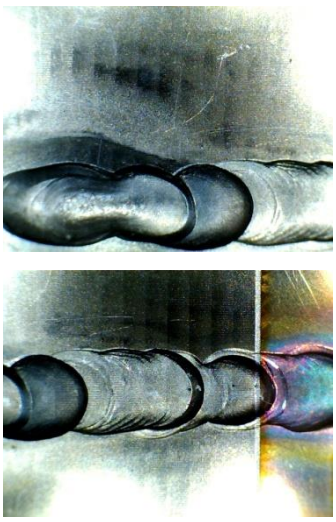

Fig. 7. Welding seam laser cleaned at f=2 kHz, τ=120 ns, P=20%, 20X magnification

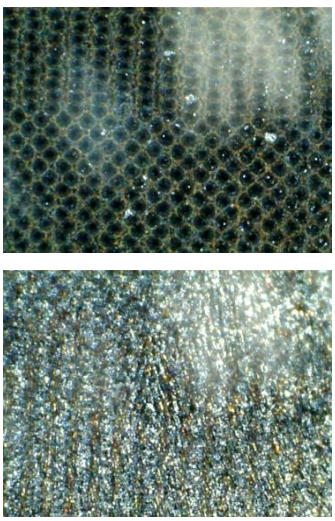

Fig. 8. Welding seam laser cleaned at f= 2 kHz, τ=120 ns, P=20%, 400X magnification

The above Figs. (5 to 8) ilustrate the best results obtained during the second batch of tests, observed at a magnification of 20X and 400X. Pulse durations of 100 ns and 120 ns at an optical output power of 20% (approximately 4W) produced the lowest values of roughness, as opposed to 80 ns pulses, at the same laser average power.

Table 6. Results of varying R_r at τ=80 ns, P=20%

R_r(kHz)	V(m/s)	V_J(m/s)	τ(ns)	P(%)	R_a(μm)
5	0.342	1.026	80	20	0.28
10	0.684	2.052			0.18
15	1.026	3.078			0.28
20	1.368	4.104			0.20
25	1.711	5.133			0.22
30	2.053	6.159			0.37

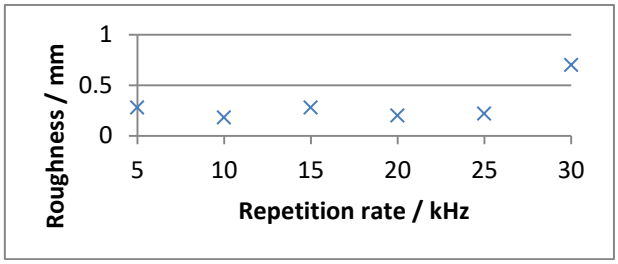

Fig. 9. Plot of R_a against R_r at τ=80 ns, P=20

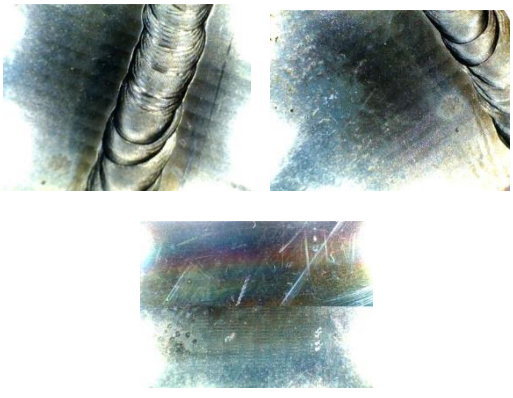

Fig. 10. Welding seam laser cleaned at f=2 kHz, τ=120 ns, P=20%, 20X magnification

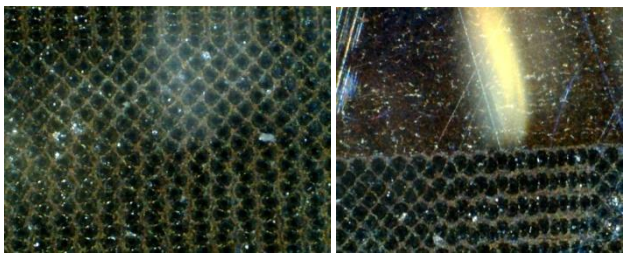

Fig. 11. Welding seam laser cleaned at f=2 kHz, τ=80 ns, P=20%, 400X magnification

Table 7. Results of varying R_r at τ=80 ns, P=30%

R_r(kHz)	V(m/s)	V_J(m/s)	τ(ns)	P(%)	R_a(μm)
5	0.342	1.026	80	30	0.64
10	0.684	2.052			0.73
15	1.026	3.078			0.47
20	1.368	4.104			0.66
25	1.711	5.133			0.32
30	2.053	6.159			0.38
35	2.395	7.185			0.28

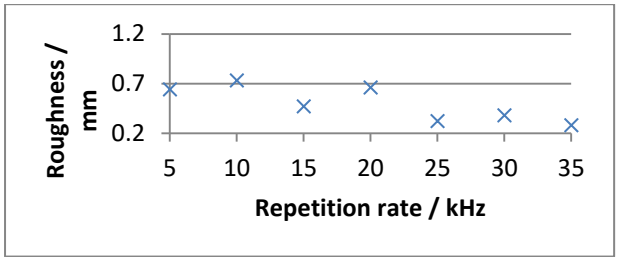

Fig. 12. Plot of R_a against R_r at τ=80 ns, P=30%

Table 8. Results of varying R_r at τ=100 ns, P=30%

R_r(kHz)	V(m/s)	V_J(m/s)	τ(ns)	P(%)	R_a(μm)
5	0.342	1.026	100	30	0.59
10	0.684	2.052			0.6
15	1.026	3.078			0.5
20	1.368	4.104			0.52
25	1.711	5.133			0.19
30	2.053	6.159			0.15
35	2.395	7.185			0.13

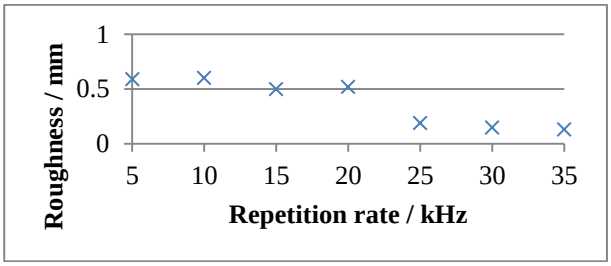

Fig. 13. Plot of R_a against R_r at τ=100 ns, P=30%

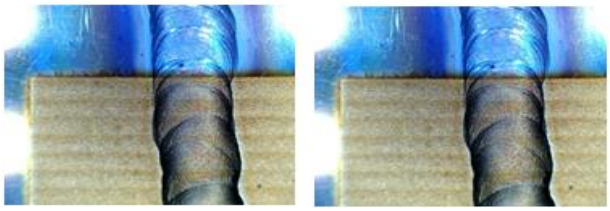

Fig. 14. Welding seam laser cleaned at f=2 kHz, τ=120 ns, P=100%, 20X magnification

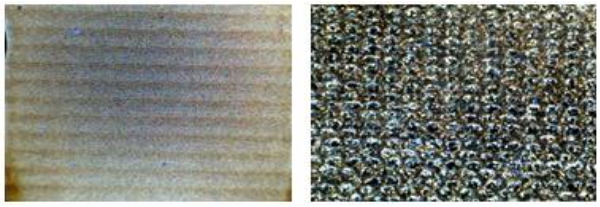

Fig.15. Welding seam laser cleaned at f=2 kHz, τ=120 ns, P=100%, 400X magnification

Table 9. Results of varying R_r at τ=120 ns, P=30%

R_r(kHz)	V(m/s)	V_J(m/s)	τ(ns)	P(%)	R_a(μm)
5	0.342	1.026	120	30	0.17
10	0.684	2.052			0.24
15	1.026	3.078			0.34
20	1.368	4.104			0.24
25	1.711	5.133			0.97
30	2.053	6.159			0.27
35	2.395	7.185			0.18
37	2.532	7.596			0.35

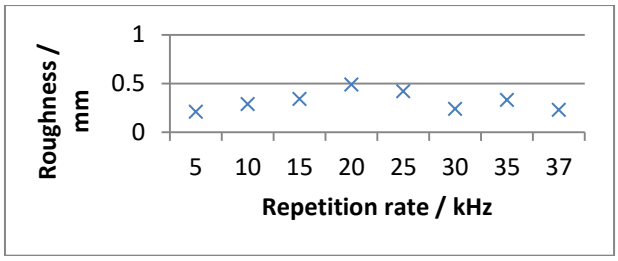

Fig. 16. Plot of R_a against R_r at τ=120 ns, P=30%

Table 10. Results of varying R_r at τ=80 ns, P=40%

R_r(kHz)	V(m/s)	V_J(m/s)	τ(ns)	P(%)	R_a(μm)
5	0.342	1.026	80	40	0.48
10	0.684	2.052			0.62
15	1.026	3.078			0.42
20	1.368	4.104			0.52
25	1.711	5.133			0.53
30	2.053	6.159			0.24
35	2.395	7.185			0.17
37	2.532	7.596			0.23

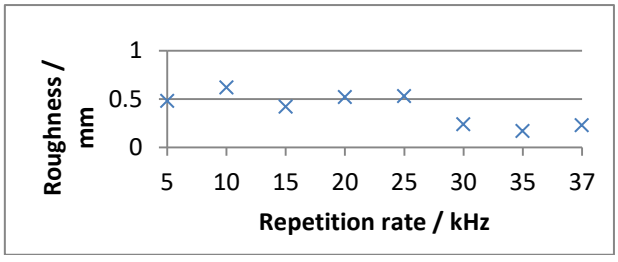

Fig. 17. Plot of R_a against R_r at τ=80 ns, P=40%

Table 11. Results of varying R_r at τ=100 ns, P=40%

R_r(kHz)	V(m/s)	V_J(m/s)	τ(ns)	P(%)	R_a(μm)
5	0.342	1.026	100	40	0.6
10	0.684	2.052			0.71
15	1.026	3.078			0.63
20	1.368	4.104			0.69
25	1.711	5.133			0.6
30	2.053	6.159			0.86

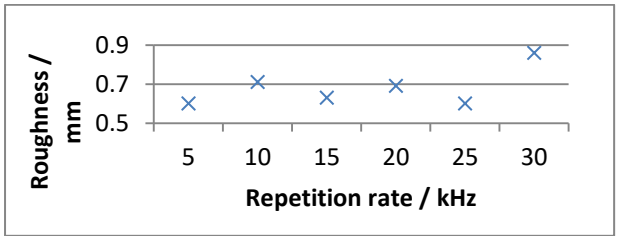

Fig. 18. Plot of R_a against R_r at τ=100 ns, P=40%

Table 12. Results of varying R_r at τ=120 ns, P=40%

R_r(kHz)	V(m/s)	V_J(m/s)	τ(ns)	P(%)	R_a(μm)
5	0.342	1.026	120	40	0.39
10	0.684	2.052			0.53
15	1.026	3.078			0.68
20	1.368	4.104			0.69
25	1.711	5.133			0.28
30	2.053	6.159			0.22
35	2.395	7.185			0.21
37	2.532	7.596			0.2

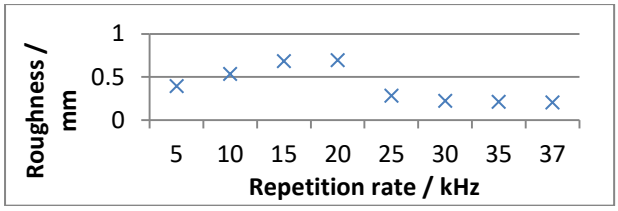

Fig. 19. Plot of R_a against R_r at τ=120 ns, P=40%

4. Conclusion

Using the machine presented above, the laser ablation of oxides resulting from the exposure of alloyed steels to high temperatures has been successfully achieved at an acceptable working speed and processing time, despite the use of a low-power fiber laser generator.

Considering both batches of tests, the working parameters that gave a roughness value of less than 0.2 microns, depending on the laser output power, are: at 20%, with 5 kHz and 100 ns pulse duration, 10 kHz and 120 ns pulse duration, 10 kHz and 80 ns pulse duration; at 30% output power: 25kHz/30kHz/35kHz with 100 ns pulse duration, 5 kHz/35 kHz with 120 ns pulse duration; at 40% output power: 35 kHz with 80 ns pulse duration.

A good observation would be that the real value of the spot diameter is less than the theoretical value. Thus, uncleaned areas occur between raster lines, an undesirable effect for some applications. This can be avoided either by decreasing the distance between the raster lines by applying a correction factor at the time of calculation (it will be necessary to determine this correction factor) or by a vertical and horizontal scanning of the area to be cleaned (which would lead, in theory, to the minimization of the uncleaned area, not its complete elimination).

References

[1] O. Dontu, S. Ganatsios, M. Covrig, Revista de Chimie **56**(3), 322 (2005).
[2] O. Turcan, O. Dontu, J. L. O. Moreno, I. Voiculescu, D. Savastru, I. M. Vasile, J. Optoelectron. Adv. M. **16**(1-2), 20 (2014).
[3] O. Dontu, S. Ganatsios, N. Alexandrescu, C. Predescu, Proceedings of the Institution of Mechanical Engineers, Part C: Journal of Mechanical Engineering Science **219**(8), 823(2005).
[4] S. V. Savu, I. D. Savu, G. C. Benga, I. Ciupitu, Optoelectron. Adv. Mat. **10**(9-10), 752 (2016).
[5] D. Popa, I. R. Bordea, A. V. Burde, B. Crisan, R. S. Campian, M. Constantiniuc, Optoelectron. Adv. Mat. **10**(9-10), 785 (2016).
[6] C. Cosma, N. Balc, M. Moldovan, L. Morovic, P. Gogola, C. Miron-Borzan, J. Optoelectron. Adv. M. **19**(11 – 12), 738 (2017).
[7] A. Pascu, E. M. Stanciu, D. Savastru, V. Geanta, C. Croitoru, J. Optoelectron. Adv. M. **19**(1-2), 66 (2017).
[8] E. Moraru, O. Dontu, A. Petre, D. Vaireanu, F. Constantinescu, D. Besnea, J. Optoelectron. Adv. M. **20**(3- 4), 208 (2018).
[9] H. Gu, X. Chen, J. Zhao, J. Optoelectron. Adv. M. **19**(11- 12), 693 (2017).
[10] H. Lin, P.Zhao, C. Guo, C. Li, Z. Li, Z. Huang, X. Tang, J. Optoelectron. Adv. M. **11**(5-6), 277 (2017).
[11] A. Z. Zulkifli, N. A. Abdul Kadir, E. I. Ismail, M. Yasin, Z. Jusoh, H. Ahmad, S. W. Harun, J. Optoelectron. Adv. M. **19**(3 - 4), 127 (2017).
[12] H. Lin, X. Tang, P. Zhao, C. Guo, Z. Huang, Z. Li, C. Li, Optoelectron. Adv. Mat. **11**(3-4), 131 (2017).
[13] H. Shamsudin, A. A. Latiff, N. N. Razak, Z. Jusoh, H. Ahmad, S. W. Harun, J. Optoelectron. Adv. M. **18**(9-10), 757 (2016).
[14] T. Ohnishi, T. Yamamoto, S. Meguro, H. Koinuma, M. Lippmaa, Journal of Physics: Conference Series **59**, 514 (2007).
[15] K. Chongcharoen, P. Kittiboonanan, A. Ratanavis, Siam Physics Congress 2017 (SPC2017), IOP Conf. Series: Journal of Physics: Conf. Series **901**, (2017).
[16] Yong-Feng Lu, Wen-Dong Song, Ming-Hui Hong, Zhong-Min Ren, Qiong Chen, Tow-Chong Chong, Japanese Journal of Applied Physics, Part 1: Regular

Papers and Short Notes and Review Papers **39**, 8 (2000).
[17] Yong-Feng Lu, Yoshinobu Aoyagi, Mikio Takai, Susumu Namba, Japanese Journal of Applied Physics, Part 1: Regular Papers and Short Notes and Review Papers **33**, 12S (1994).
[18] Pandora Psyllaki, Roland Oltra, Materials Science and Engineering: A **292**, 1-2 (2000).
[19] SCANLAB AG http://www.scanlab.de/sites/default/files/PDF-Dateien/Data-Sheets/RTC5-EN.pdf
[20] IPG Photonics - "YLP-V2-100-20-20 manual "
[21] Thorlabs Inc "F-Theta Lenses Tutorial" https://www.thorlabs.de/newgrouppage9.cfm?objectgroup_id=10766
[22] SPI Lasers UK Ltd, Laser Processing Applications – Laser Cleaning: http://www.spilasers.com/laser-processing-applications/laser-cleaning
[23] UNITEK MIYACHI CORPORATION – "Nd:YAG Laser Welding Guide", 2003 http://www.amadamiyachieurope.com/cmdata/documents/Laser-Welding-fundamentals.PDF

*Corresponding author: m.selagea@yahoo.com, d_bes@yahoo.com; eddy_milan91@yahoo.com